

Interannual variability of deep convection over the tropical warm pool

Shuyi S. Chen and R. A. Houze, Jr.

Department of Atmospheric Sciences, University of Washington, Seattle

Abstract. Satellite data show that the total amount of deep convection was nearly constant from year to year over the “warm pool” region of the tropical Indian and Pacific oceans, but the spatial distribution varied. In the 1986–1987 warm El Niño/Southern Oscillation event, the maximum of deep convective activity was over the high sea surface temperature (SST) of the west central Pacific, with a local minimum over the eastern Indian Ocean. In the 1988–1989 cold ENSO event the maximum convective activity switched to the eastern Indian Ocean, with a minimum over the west central Pacific. The SST changed very little over the eastern Indian Ocean from year to year, and the centers of convective activity were always collocated with the four-month mean low-level westerlies in each year. The latitude of the cloudy region of the intraseasonal oscillation (ISO) varied interannually. The interannual differences in deep convective activity over the warm pool were accounted for almost exclusively by the occurrence or nonoccurrence of extremely large, long-lasting, deep mesoscale cloud systems (cloud tops < 208 K with horizontal dimensions ~300–700 km). Such cloud systems occurred more frequently than normal over the western Pacific during the warm ENSO event and over the eastern Indian Ocean during the cold event. They occurred more frequently over the tropical eastern Indian and western Pacific oceans than over the maritime continent, thus accounting for the seesaw pattern of the observed cold cloudiness between the two oceanic regions on both interannual and intraseasonal timescales.

1. Introduction

The tropical Indian and western central Pacific oceans experienced both extremes of the El Niño/Southern Oscillation (ENSO) cycle during 1986–1989. Warm episode conditions were observed during much of late 1986 through early 1987; near-normal conditions were observed during late 1987 to mid-1988; and an impressive cold phase began in mid-1988 and continued through mid-1989. A pronounced interannual variability of both high cloudiness and rainfall were observed, especially over the western central Pacific.

Janowiak and Arkin [1991] examined the rainfall variations derived from satellite infrared (IR) data for the 1986–1989 period. They found that the largest difference in global tropical rainfall from year to year occurred over the tropical central Pacific at 175°W. Surface observations of rainfall have also shown a significant interannual variability in the Pacific basin related to the ENSO cycles [Ropelewski and Halpert, 1987; 1989]. Mapes and Houze [1993] examined the climatology of the cloud clusters defined by cold cloud temperature from satellite IR data for the same three-year time period. They found no significant changes from year to year in overall characteristics of the cloud population over the Indo-Pacific warm-pool region.

The most prominent large-scale feature over the warm pool is the convective variability associated with the tropical intraseasonal oscillation (ISO), which has a 30–60 day timescale. The ISO is characterized as a slow eastward propagation of anomalous equatorial westerlies and easterlies

in the lower and upper troposphere, respectively [Madden and Julian, 1971, 1972], and is also known as the Madden-Julian Oscillation. Accompanying the eastward propagation of anomalous zonal wind is an eastward propagation of a large-scale region of anomalously frequent deep convection [e.g., Lau and Chan, 1985; Knutson and Weickmann, 1987; Wang and Rui, 1990]. The eastward-propagating convective anomaly typically originates in the Indian Ocean, weakens as it moves across the maritime continent (Indonesia and Malaysia, Ramage [1971]) and re-amplifies in the western Pacific warm-pool region. The deep convection comprising the large-scale convective anomaly associated with the ISO exhibits a rich multiscale temporal and spatial variability [Nakazawa, 1988; Lau et al., 1991; Sui and Lau, 1992; Hendon and Liebmann, 1994; Chen et al., 1996]. The large-scale circulation of the ISO interacts with high-frequency disturbances (such as two-day inertio-gravity waves) and convective organization of individual convective systems [e.g., Chen and Houze, 1997].

Although theories have attempted to explain the eastward propagation of the ISO in terms of mobile wave-conditional stability of the second kind (CISK, Charney and Eliassen [1964]) [Lau et al., 1989], evaporation-wind feedback [Emanuel, 1987; Neelin et al., 1987], frictional convergence in the atmospheric boundary layer [Wang, 1988; Salby et al., 1994], radiative-convective interaction [Hu and Randall, 1994], and convective discharge-recharge [Hendon, 1988], the mechanisms for this phenomenon need to be further verified. Other observational studies have shown the importance of the equatorial Rossby waves [Nogués-Paegle et al., 1989] and the influence of the extratropics [e.g., Hsu et al., 1990; Kiladis and Weickmann, 1992].

An interesting feature of the ISO is an out-of-phase relationship between the convective anomalies over the Indian

Copyright 1997 by the American Geophysical Union.

Paper number 97JD02238.
0148-0227/97/97JD-02238\$09.00

Ocean and the western Pacific, as discussed by *Zhu and Wang* [1993]. They used the term “seesaw” for the dipole pattern. They showed that the seesaw forms as a result of the longitudinal variation of the eastward-propagating large-scale ISO cloud ensemble, which strongly amplifies in the equatorial Indian Ocean, weakens over the maritime continent, and reintensifies in the South Pacific Convergence Zone (SPCZ).

Several studies have shown composites of ISO structure and life cycle [*Knutson and Weickmann*, 1987; *Rui and Wang*, 1990; *Hendon and Salby*, 1994]. *Gutzler* [1991] explored the interannual variation of equatorial zonal winds associated with the ISO. The convective variability among individual ISOs, especially in different ENSO conditions, has not been investigated. Case studies of the ISO [e.g., *Weickmann and Khalsa*, 1990] revealed many interesting features of each ISO within a particular large-scale flow regime. The influence of various climatological conditions on the deep convection associated with the ISO over the warm pool in relation to the ENSO cycle has not been examined.

The objective of this paper is to examine the spatial and temporal variations of the deep convective activity over the tropical Indo-Pacific warm-pool region during the rainy seasons of November–February 1986–1989 and these variations in relation to the interannual variation of the ENSO conditions. Special focus is on the intraseasonal time and space scales and on the characteristics of the cloud systems accounting for the interannual variability.

2. Date and Method of Analysis

2.1. Data

We use 3-hourly infrared (IR) images from the Japanese Geosynchronous Meteorological Satellite (GMS-3) with about 10-km resolution (with highest resolution of 9 km at the subsatellite point $\sim 0^\circ$ and 140°E) as the primary data set to examine the variation of cold cloud tops over the Indo-Pacific warm-pool region (80°E – 160°W and 20°N – 20°S). The data were archived as an International Satellite Cloud Climatology Project (ISCCP) B-1 product and were obtained from the National Oceanic and Atmospheric Administration (NOAA) Satellite Data Services Division. The oceanic precipitation is estimated on a 2.5° grid from the microwave sounding unit (MSU) channels 1–3 data on the TIROS-N series of NOAA weather satellites [*Spencer*, 1993]. The European Centre for Medium-Range Forecasts (ECMWF) uninitialized global wind analysis fields at 0000 and 1200 UTC and the National Centers for Environmental Prediction (NCEP) global SST analysis are used to characterize the large-scale conditions. Both the wind and the SST data are on a 2.5° grid resolution.

2.2. Wind and Anomaly Fields

The anomaly of the horizontal wind is defined as

$$\bar{v}' = \bar{v} - \bar{V}$$

where \bar{V} is the three-month running mean and \bar{v} is the analysis. \bar{v}' is the anomaly with low frequencies, including interannual and annual cycle, removed. The three-month running mean is computed with a weighted filter which decreases smoothly and symmetrically outward from the center following a normal probability curve with a frequency response of half power at about 150 days. We use \bar{v}' to represent intraseasonal and higher frequency modes.

2.3. Percent High Cloudiness

We present four-month-average satellite-observed cloud coverage in terms of the percent high cloudiness (PHC), which is the fractional coverage (in time or space) of cloud with IR temperature less than a given threshold. The four-month-average hourly PHC is calculated as the percentage of images colder than the threshold temperature at each pixel. PHC indicates both temporal and spatial distribution of deep convection. PHC_{235} will be used to denote the fractional coverage of clouds with IR temperature < 235 K. The 235 K threshold was used in global rainfall estimates by *Arkin and Meisner* [1987] and *Janowiak and Arkin* [1991].

2.4. Cloud Cluster Identification

We define a cloud cluster as a region at an instant of time within a single closed isotherm of threshold temperature T_{th} in which the infrared temperature is $< T_{th}$. To identify a cluster at a particular time, connected segments of cold cloudiness (cloud-top temperature $< T_{th}$) are found within each line (latitude row) of the data array containing one satellite image. A connected segment of $< T_{th}$ is called a line cluster. The line clusters in two successive lines must share a column (not merely touch diagonally) to be considered connected from one line to the next. A set of line clusters connected from one line to the next constitutes one cloud cluster. Each cloud cluster is then characterized by its area and centroid position. In this study, we use an infrared temperature threshold of $T_{th} = 208$ K to identify all the cloud clusters in the field of view of the GMS domain. The 208 K threshold is a close approximation to the boundary of the precipitating core of tropical deep convective systems over the western Pacific. While arbitrary, it is a rather conservative indicator of precipitating deep convection. This cloud cluster analysis has been used in *Williams and Houze* [1987], *Mapes and Houze* [1993], *Chen et al.* [1996], and *Chen and Houze* [1997].

3. Time-Mean Features

We use the notation “NDJF” to refer to the rainy (or wet) season, which occurs from November through February in the equatorial Indo-Pacific warm-pool region, although the rainy season over the equatorial warm pool is usually from October to March. In this section, we compare time-mean features of SST, PHC, rainfall, and low- and high-level winds in the GMS domain (80°E – 160°W , 20°N – 20°S) during the three NDJFs from 1986–1987 to 1988–1989. A full ENSO cycle occurred during the three-year period, with a warm event in 1986–1987, a transitional year in 1987–1988, and a cold event in 1988–1989. Measured by the Southern Oscillation Index (SOI), (defined as the difference between the standardized sea level pressure anomaly at Tahiti and Darwin, see *Ropelewski and Jones*, [1987]), the warm event reached its mature phase in April 1987 and the cold event reached its extreme condition in October–November 1988 [*Climate Analysis Center*, 1989]. In the eastern equatorial Pacific region known as Niño-3 (5°N – 5°S , 150°W – 90°W), which is out of the GMS domain, the SST anomaly associated with the warm event did not reach its maximum until the second half of 1987 [*Hayes et al.*, 1991]. Over the equatorial area of the western central Pacific (5°N – 5°S , 160°E – 160°W) the maximum positive convective anomaly associated with the warm event, inferred from the standard

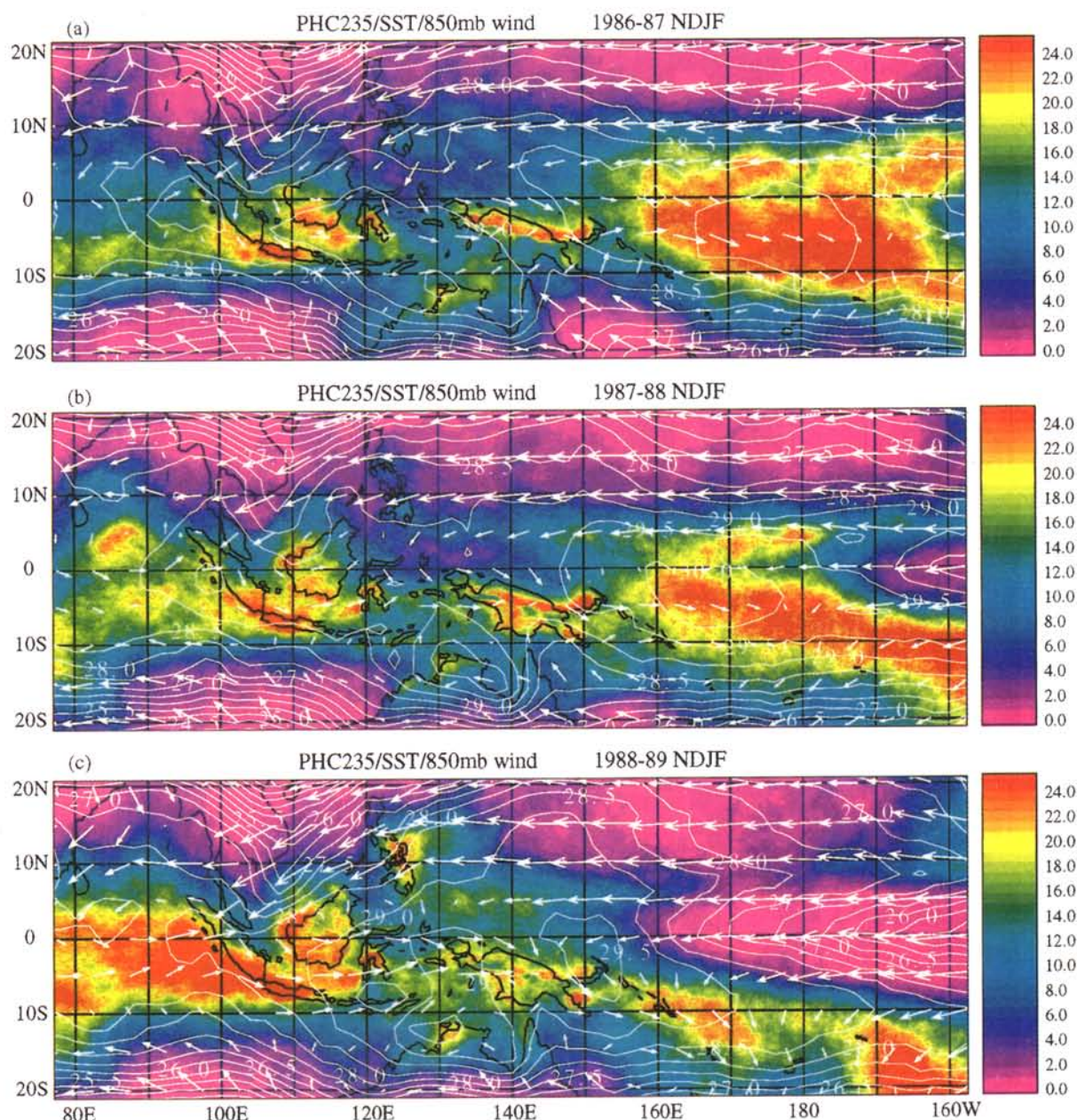


Plate 1. The percent high cloudiness (PHC₂₃₅, the fractional coverage of cloud with IR temperature < 235 K) is overlaid with the mean (NCEP SST) and the mean (ECMWF) global 850-mbar wind analysis over the Indo-Pacific warm pool for November-February, (a) 1986-1987, (b) 1987-1988, and (c) 1988-1989. A 10 m s⁻¹ wind is represented by a vector 2.5° in length on the map.

deviation of monthly mean outgoing longwave radiation (OLR), took place during December 1986 to February 1987. The maximum negative convective anomaly over the same area occurred in November 1988 to January 1989 [Climate Analysis Center, 1989].

3.1. Sea Surface Temperature

The NDJF-mean SST (contours in Plate 1) shows the warm pool (SST ≥ 28.5°C) in the eastern Indian and western Pacific oceans. The most drastic variability of the warm pool from year to year is the zonal displacement of its eastern boundary near the equator. In NDJF of 1986-1987 and 1987-1988 (Plates 1a and 1b) the warm pool extended eastward as far as 160°W

and the highest SST was located east of 160°E. In 1988-1989 the cold tongue penetrated along the equator from the east and the warm pool near the equator retreated to the west of the dateline (Plate 1c); a relatively warm body of water can nevertheless be found south of the cold tongue near the dateline. The SST differences in the equatorial region near the dateline between the NDJFs of 1986-1987/1987-1988 and that of 1988-1989 are as large as 3°C (Plate 1), similar to the in situ measurement from a Tropical Ocean Global Atmosphere Tropical Atmosphere and Ocean (TOGA TAO) buoy at 0°, 165°E [Kessler et al., 1996].

The SST variability over three years is much less significant in the region surrounding the maritime continent

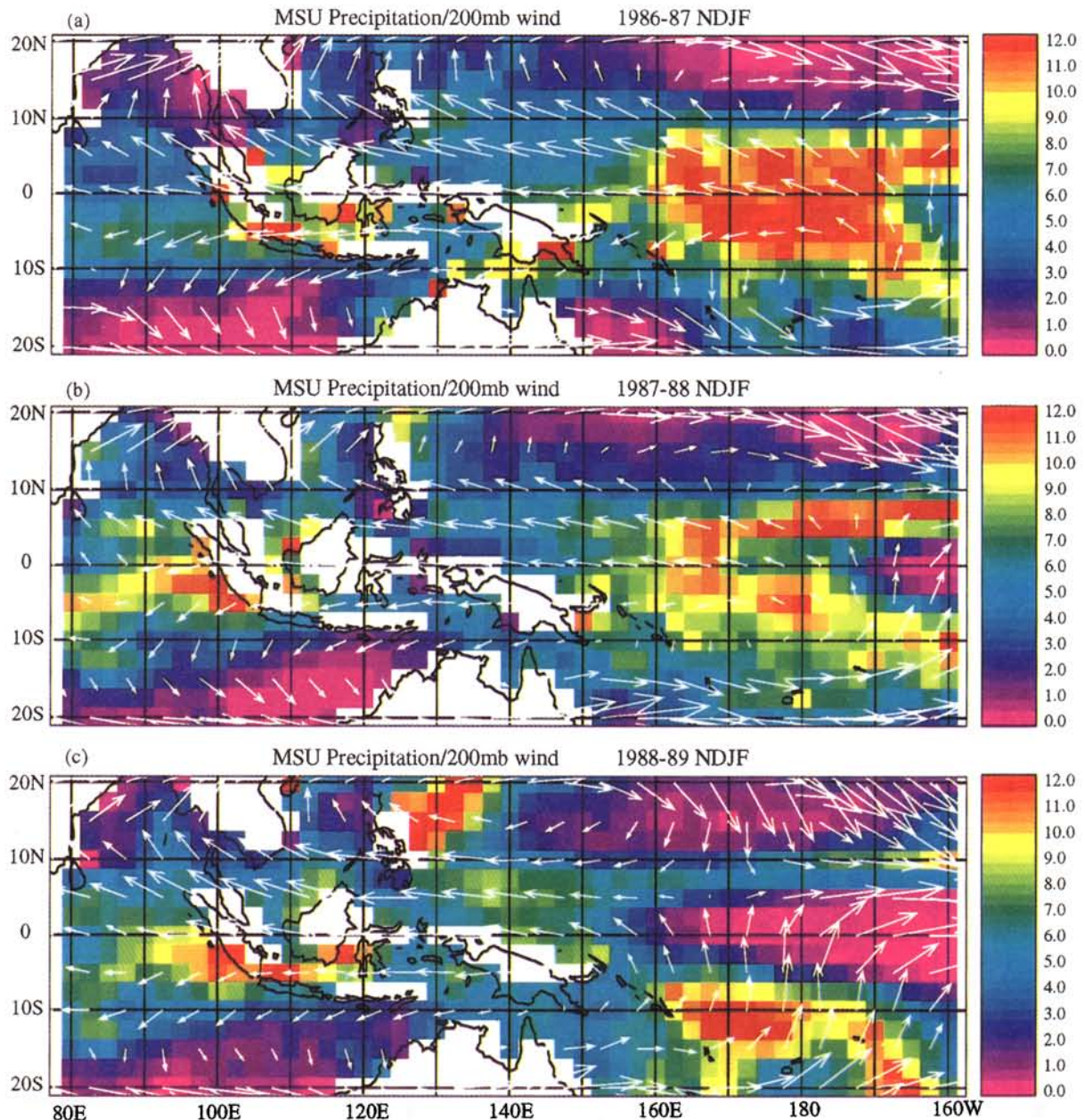


Plate 2. The Microwave sounding unit (MSU) estimated precipitation overlaid with the mean ECMWF global 200-mbar wind analysis, for the same time periods as in Plate 1. Wind vector scale as in Plate 1.

and in the eastern Indian Ocean. There, year-to-year changes in the NDJF-mean SST are in general about 0.5°C .

3.2. PHC and Rainfall

Colors in Plate 1 show distributions of NDJF-mean PHC_{235} over the equatorial GMS domain. The contrasts between the 1986-1987 warm ENSO event and the 1988-1989 cold ENSO event in the western central Pacific region (150°E - 160°W) and in the eastern Indian Ocean are striking. In general, the largest convective region was located near the equator in the western central Pacific (near the dateline) in 1986-1987 and 1987-1988 but shifted to the eastern Indian Ocean in 1988-1989. In the western central Pacific the vigorous convective activity near the equator (0° - 10°S) in 1986-1987 and 1987-1988 almost completely disappeared in 1988-1989 when the cold

tongue replaced the warm pool in that region. Deep convection, less frequent but still significant, shifted to the south of the cold tongue over the relatively warm water. There, the convective distribution indicates a distinct SPCZ. In the region of the maritime continent, mean deep convection remained relatively weak (more scattered, concentrated only over land), even in the region of the Australian summer monsoon (northernmost Australia), and underwent less year-to-year fluctuation.

Many studies have attempted to relate satellite-observed variability of deep convection to SST in the tropics [e.g., *Graham and Barnett*, 1987; *Fu et al.*, 1990; *Zhang*, 1993]. Comparisons of PHC and SST distributions in Plate 1 indicate no simple SST-convection relationship. In the western Pacific the most frequent deep convection was located over the warmest water in 1986-1987 and 1987-1988 but became much

less frequent and shifted to the south over the relatively warm water in 1988-1989 when the equatorial warm pool was replaced by the cold tongue. On the other hand, deep convection in the region surrounding the maritime continent was less frequent than over the western Pacific or over the eastern Indian Ocean regardless of the SST distributions. Deep convection in the eastern Indian Ocean was much more frequent in 1988-1989 than the other two years, even though the SST did not change much. In fact, the most frequent deep convection in 1988-1989 was located west of the warmest sea surface. These results suggest that although deep convection prefers open, warm oceans, the large-scale distribution of deep convection does not follow the SST distribution precisely in the equatorial Indo-Pacific warm-pool region.

The NDJF-mean oceanic precipitation estimate based on the MSU data is displayed by the colors in Plate 2. The precipitation patterns are in general similar to those of the PHC_{235} over the western Pacific for all three wet seasons. In the eastern Indian Ocean, precipitation increased from the relative minimum in 1986-1987 to the higher values in the later two years, although its maximum in 1988-1989 was not as pronounced as the PHC_{235} shown in Plate 1. The year-to-year variability over the warm pool shown in Plates 1 and 2 has contributed to the global tropical zonal average (from 21.25°N to 21.25°S) rainfall anomaly maxima near the equator in 1986-1987 and south of the equator between 10° and 20°S in 1988-1989, as discussed by Janowiak and Arkin [1991, Figure 9].

3.3. Winds

The NDJF mean wind vectors at 850 and 200 mbar based on the ECMWF analysis are superimposed on Plates 1 and 2, respectively. The mean low-level (850 mbar) equatorial zonal wind (Plate 1) was predominantly westerly over most of the GMS domain between 0° and 10°S except in 1988-1989 where strong easterlies penetrated into the domain from the east over the cold tongue region. Strong 850-mbar westerlies were collocated with the most convectively active regions: in the western central Pacific in 1986-1987 and 1987-1988 and in the eastern Indian Ocean in 1988-1989. No mean low-level easterlies with comparative strength were found to the east of a convective center in the eastern Indian Ocean in 1988-1989. A similar collocation of a low-level westerly and convective

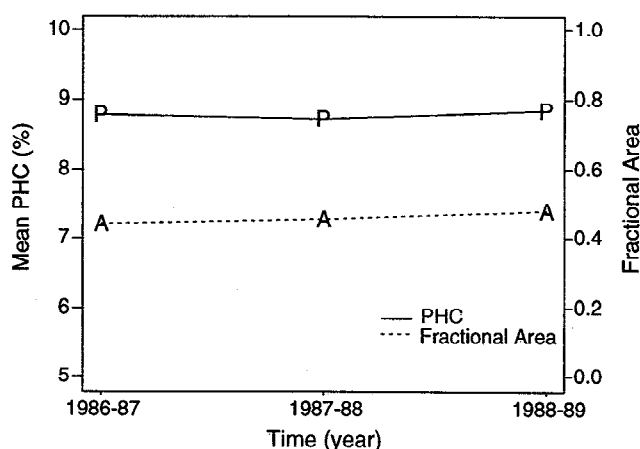


Figure 1. Domain-averaged four-month mean PHC_{235} (line A) and fractional coverage of the area of PHC_{235} greater than 8.5 (line P) for the three wet seasons as in Plate 1.

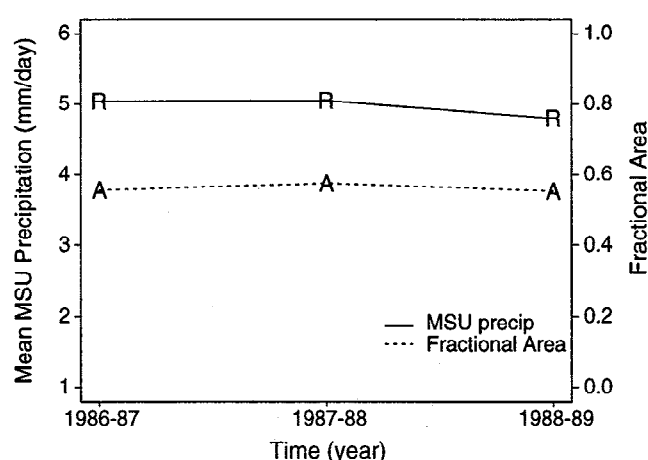


Figure 2. Domain-averaged four-month mean MSU-estimated precipitation (line R) and fractional coverage of the area of MSU-estimated precipitation greater than 4.5 (mm/d) (line A) for the three wet seasons as in Plate 2.

activity center is also found on the intraseasonal time and space scales and is in Section 4. In 1988-1989 there is no mean low level easterlies on the east side of the maximum convective center (heat source) over the eastern Indian Ocean (Plate 1c). The low-level westerlies extended about 40° of longitude farther east of the heat source. This pattern is somewhat different than that predicted by simple, linear steady-state atmospheric models, such as that of Gill [1980], in which winds are forced by a prescribed isolated heat source. (To compare with model results, the observed zonal winds can be viewed as perturbations to the mean since the annual mean zonal wind in the domain of interest is very weak.) Using multiple heat sources based on observations and an improved vertical heating profile which includes the effect of mature mesoscale convective systems, Hartmann *et al.* [1984] were able to get a more realistic vertical structure of the Walker circulation with a westward tilt in a linear steady-state model. However, the low-level easterly branch was still too far west (relative to the heat center) in their model compared to the observations over the warm pool [Newell *et al.*, 1974].

The upper-level (200 mbar) equatorial zonal wind over the warm pool was dominated by mean easterlies, with the exception of 1988-89 over the western central Pacific (Plate 2). The 200-mbar equatorial mean easterlies were only observed from 155°E to the Indian Ocean in 1988-1989, which is collocated with the extended 850-mbar westerlies (Plates 1c and 2c). A strong cross-equatorial flow occurred over the cold tongue region in 1988-1989 when convection was absent there (Plate 2c). A similar northerly cross-equatorial flow was evident to the east of the convective center over the central Pacific in 1986-1987 and 1987-1988 (Plates 2a and 2b).

3.4. Total Domain-Averaged PHC and Precipitation

Despite the striking interannual variation in the spatial distributions of PHC_{235} and MSU precipitation, the total amount of deep convection over the Indo-Pacific warm-pool region (80°E-160°W and 21.5°N-21.5°S, see Plates 1 and 2) did not change much. Figures 1 and 2 show relatively constant domain-averaged PHC_{235} and MSU precipitation (solid lines) over the 4-month period for each year. The dashed lines are the

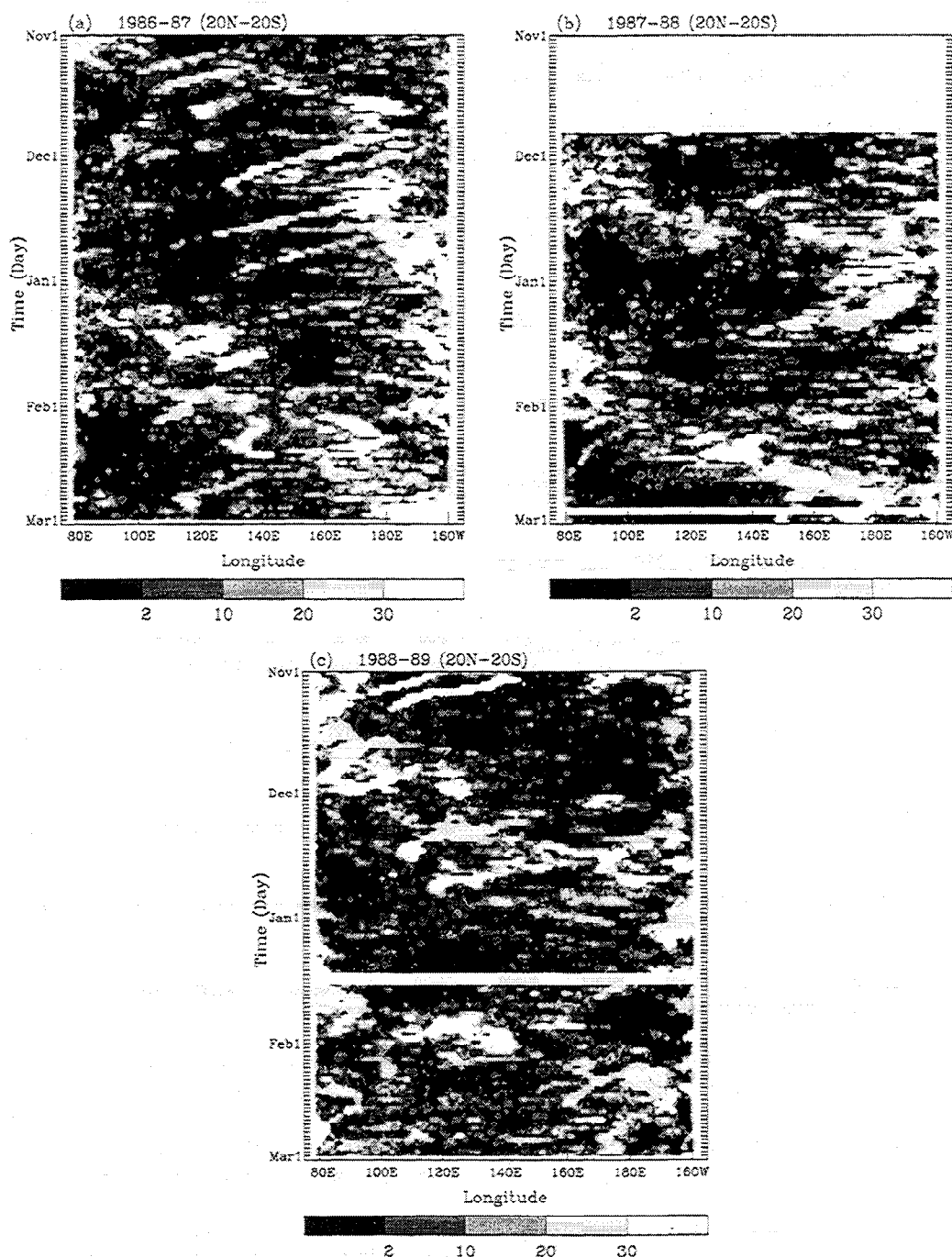


Figure 3. Time-longitude diagrams of daily PHC₂₃₅ index for (a) 1986-1987, (b) 1987-1988, and (c) 1988-1989. Each one day by 0.5° longitude grid element is shaded according to the meridional summation of the number of the elements with the daily PHC₂₃₅ greater than 20% between 20°N and 20°S.

fractional area coverage of PHC₂₃₅ > 8.5% and MSU precipitation > 4.5 mm d⁻¹, where 8.5% and 4.5 mm d⁻¹ are values close to the domain average for all three years. The fact that both total domain-averaged cold cloudiness and precipitation as well as the areal coverage of intense (above mean) deep convection were nearly constant suggests a near conservation of cold cloudiness and precipitation over the Indo-Pacific warm-pool region. This result indicates that the mechanism(s) controlling the total amount of deep convection over the warm pool may be independent of the ENSO cycle. However, it remains that the spatial shifting of the location of the convective activity center within the region, between the

western central Pacific and the eastern Indian Ocean, and between the equatorial region and the SPCZ, is the main reason for the global response to the convective variability related to the ENSO cycle.

4. Intraseasonal Oscillations During 1986-1989

4.1. Time-Longitude Variations of the ISO

During the rainy season over the warm pool (November-February), most deep convection occurs in the convectively active phases of the ISO [e.g., Nakazawa, 1988; Hendon and Liebmann, 1994; Chen *et al.*, 1996]. Figure 3 shows time-

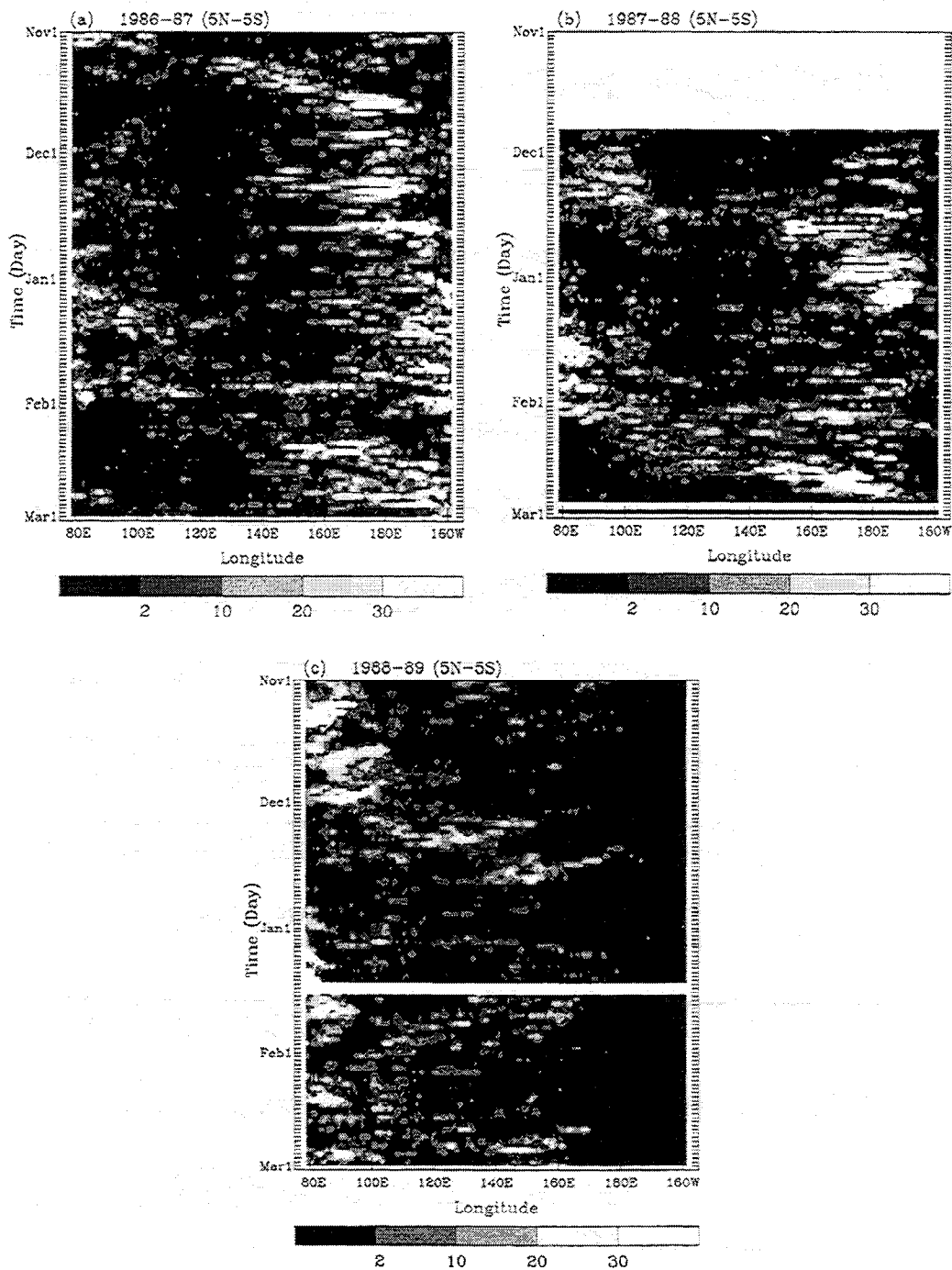


Figure 4. Same as in Figure 3, except for the equatorial band of 5°N and 5°S.

longitude plots of daily PHC_{235} histograms between 20°N and 20°S for the periods NDJF 1986-1989 from 80°E to 160°W. Each NDJF contained two cycles of ISO. Regardless of the interannual variations in the mean patterns in Plates 1 and 2, the regions of active deep convection associated with the ISO displayed very similar eastward zonal propagation in all three years. The average phase speed of the eastward-propagating cloud ensembles constituting the active phases of the ISO varied from about 3-5 m s⁻¹ in 1986-1987 (Figure 3a) to 5-7 m s⁻¹ in 1987-88 and 1988-89 (Figures 3b and 3c), similar to the 5 m s⁻¹ phase speed of an ISO composite by *Hendon and Salby* [1994].

The meridional structures of the ISO are quite different for the warm and cold ENSO events. Figure 4 shows time-longitude plots of daily PHC_{235} histograms, similar to Figure 3, but for a narrow equatorial band of 5°N-5°S. The eastward propagation of the ISO from 80°E to 160°W is similar to the time-longitude patterns over the broader latitude band in Figure 3 for 1986-1987 and 1987-1988 (Figures 4a and 4b). However, during the cold ENSO event in NDJF 1988-1989 the eastward-propagating cloud ensemble disappeared from the equatorial belt of the western central Pacific (160°E-160°W, see Figure 4c). These results indicate that although the ISO exists in the broad tropical region (20°N-20°S) during the cold event of

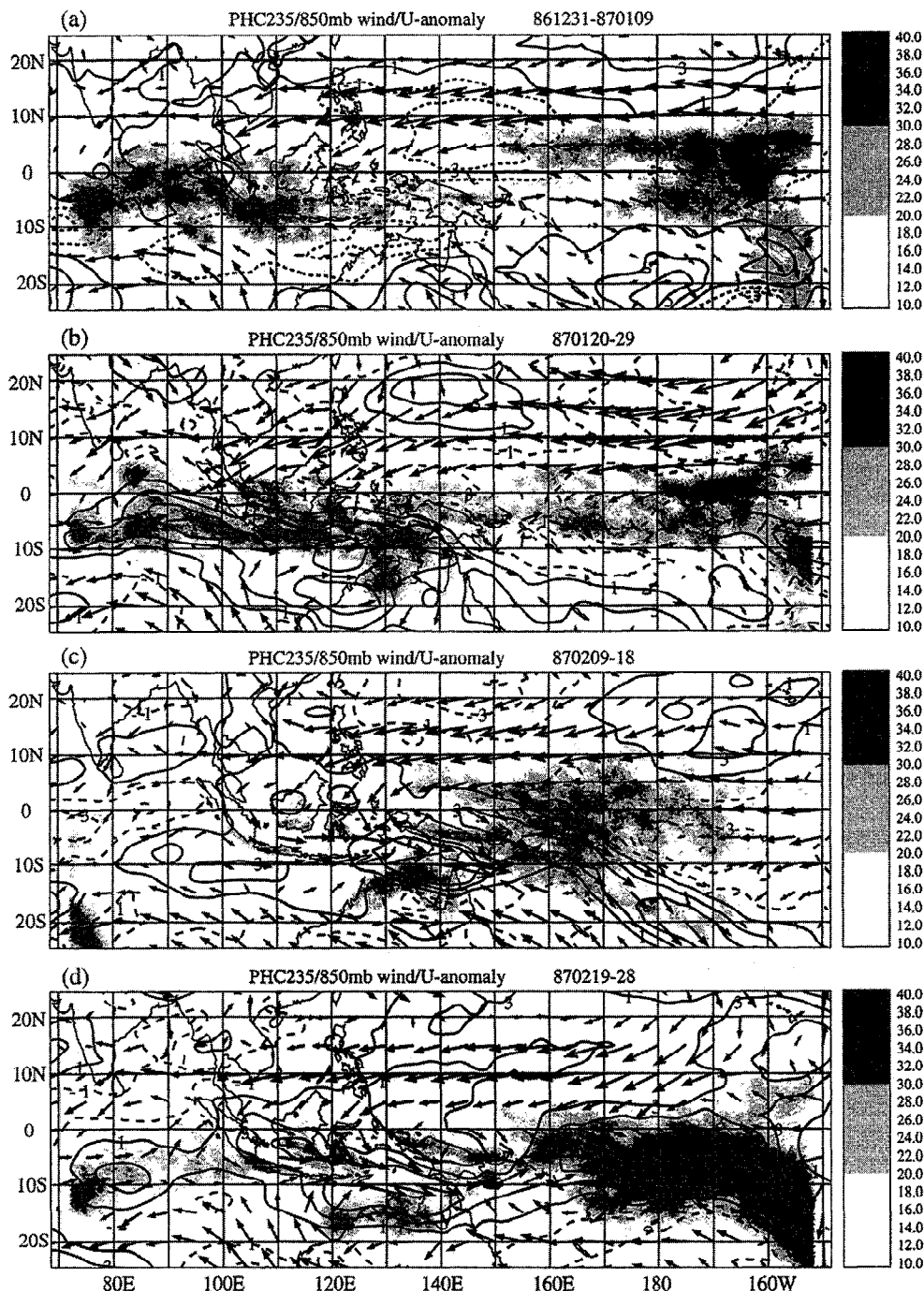


Figure 5. (a-d) Ten-day averages of PHC_{235} , the ECMWF 850-mbar wind analysis, and the 850-mbar zonal wind anomaly (contour) for the period of 31 December 1986–28 February 1987. The contour interval is 2 m s^{-1} (from -5 to 5 m s^{-1} , negative values are dashed).

1988–1989 the deep convective activity was not present over the equatorial Pacific (5°N – 5°S) (compare Figures 3c and 4c), which was dominated by the equatorial cold tongue. In NDJF 1988–1989, the cloud ensemble associated with the two ISOs was largely confined to south of the equator between 8° and 20°S during the cold ENSO event.

4.2. Equatorial Waves and the ISO

A frequently debated question is whether the atmospheric Kelvin wave plays an important role in the eastward propagation of the ISO [e.g., Emanuel, 1987; Wang, 1988;

Lau et al., 1989; Nogués-Paegle et al., 1989; Hsu et al., 1990; Hendon and Salby, 1994]. A Kelvin wave structure is defined as an eastward-propagating pair of low-level easterly and westerly wind symmetric about the equator with corresponding upper-level westerly and easterly wind [Matsuno, 1966; Gill, 1980]. Kelvin waves were often described as a forced response to convective heating and were also thought to be responsible for the eastward propagation of the ISO and associated deep convective activity in numerical modeling studies [e.g., Wang, 1988; Lau et al., 1989]. Others emphasized the importance of equatorial Rossby waves [e.g., Nogués-Paegle et

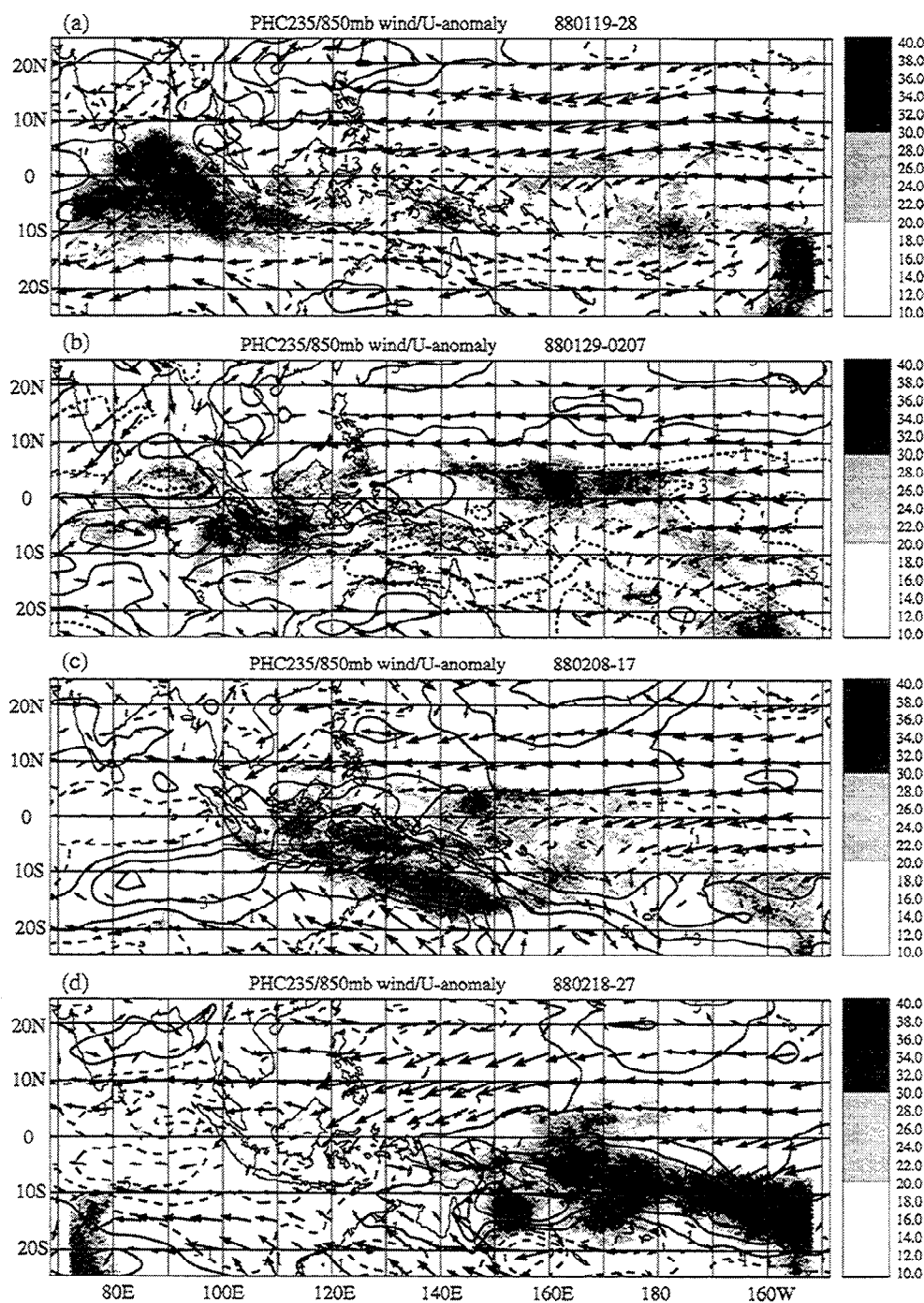


Figure 6. Same as in Figure 5, except for 19 January to 27 February 1988.

al., 1989] and influence of the extratropics [Hsu *et al.*, 1990; Kiladis and Weickmann, 1992].

Figures 5-7 show three examples of the ISO from three wet seasons in 1986-1987, 1987-1988, and 1988-1989. Each panel contains a 10-day average of the PHC_{235} (shaded), 850-mbar wind (vectors), and the u -component anomaly from the 3-month-weighted running mean (contours). The 10-day-averaged 850-mbar zonal wind anomaly indicates the circulation associated with the ISO, which excludes both the seasonal and the annual cycle as well as high-frequency influences. Two of the 10-day averages in the 1986-1987 case were omitted because of the long duration of that event.

The horizontal patterns of the eastward-propagating ISO were similar in all three cases, except the meridional shifts of the convective center over the western Pacific (compare Figures 5d and 7d). In all three cases, convective activity centers were shifted slightly south of the equator, where it is coincident with climatological convection in January and February [Hartmann and Gross, 1988].

For each ISO shown in Figures 5-7, the convective centers were mostly collocated with the low-level westerlies, similar to that found in TOGA COARE [e.g., Chen *et al.*, 1996]. Such collocation of low-level westerlies and convective activity centers was also found by others [e.g., Rui and Wang, 1990;

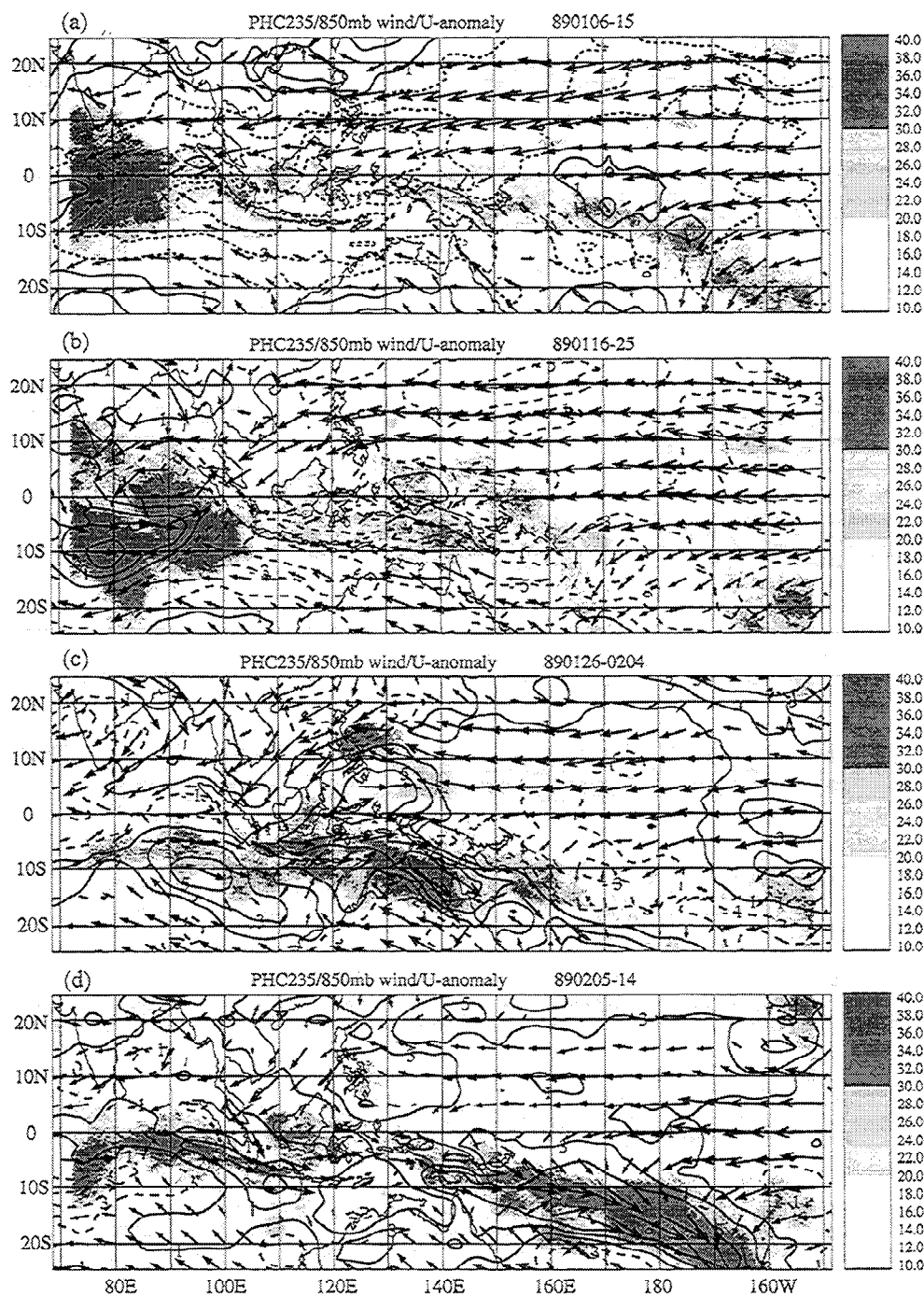


Figure 7. Same as in Figure 5, except for 6 January to 14 February 1989.

Hendon and Salby, 1994; Zhang, 1996]. The observed convective pattern is inconsistent with the mobile wave-CISK theory that predicts the convective center between the easterly and the westerly [e.g., Lau *et al.*, 1989]. The strongest low-level wind was observed in the equatorial westerlies (solid contours in Figures 5-7), not in the equatorial easterlies (dashed contours in Figures 5-7) as needed for the wind-evaporation feedback hypothesis [e.g., Emanuel, 1987; Neelin *et al.*, 1987].

The Kelvin-wave-like pattern (i.e., strong easterlies and westerlies nearly centered at the equator) is present when the ISO cloud ensemble was located near the equator (Figures 5c,

6a, and 6c). However, there is no obvious Kelvin-wave signal at low levels over the western Pacific when the convective centers lie mostly south of the equator during the cold event in 1988-1989 (Figure 7d).

The ensemble of deep convective systems associated with the ISO is more stationary and long-lasting over the eastern Indian and western Pacific oceans (Figures 5-7) than over the maritime continent, which has contributed to the seesaw pattern of the ISO. There is a significant intraseasonal variation of the intraseasonal seesaws in 1986-1989. The two poles are not balanced. The western Pacific pole is a favored location for deep convection associated with the ISO during the 1986-1987

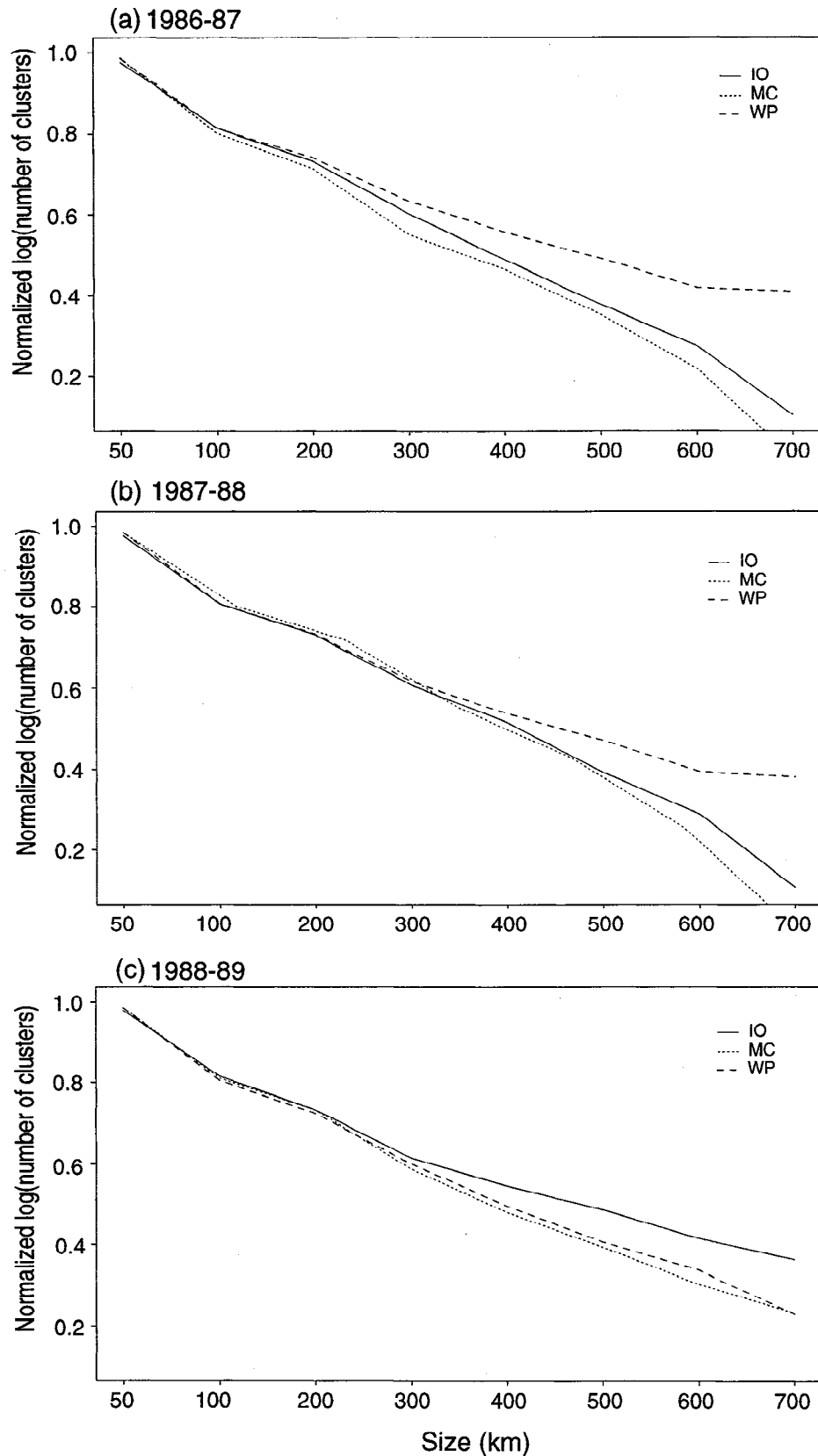


Figure 8. Normalized size distributions of number of cloud clusters (in log scale) over the Indian Ocean (IO) (solid line), the maritime continent (MC) (dotted line), and the western Pacific (WP) (dashed line) for (a) 1986-1987, (b) 1987-1988, and (c) 1988-1989.

warm ENSO event (i.e., PHC₂₃₅ in Figures 5a, 5b, and 5d), whereas the Indian Ocean is favored during the 1988-1989 cold ENSO event (Figures 7a, 7b, and 7d). This result suggests that the characteristics of the deep convection associated with the ISO contributed to the interannual variation in the NDJF-mean PHC and MSU-estimated precipitation in Plates 1 and 2.

5. Cloud Clusters

An important question is why the deep convection comprising the active phase of the ISO is more pronounced over the oceans than over the maritime continent. Is there a change in cloud population that gives rise to the anomalous PHC and precipitation accounting for the interannual variability?

In this section we examine the characteristics of the cloud clusters (or convective systems) in various regions with respect to the ENSO conditions from 1986 to 1989. Cloud clusters are defined as a closed contour surrounding a region of cloud-top temperature < 208 K on an IR satellite image (Section 2.4).

Figure 8 shows the size-frequency distributions of cloud clusters over three regions: the Indian Ocean (IO) (75°-100°E), the maritime continent (MC) (100°-145°E), and the western Pacific (WP) (145°E-160°W). (The total number of cloud clusters over the equatorial GMS domain [Plate 1] for the three years is $\sim 183 \times 10^3$, 124×10^3 , and 115×10^3 , respectively.) The frequency of small cloud clusters remained unchanged from year to year for all three regions. The largest difference is in the occurrence of the spatially large cloud clusters (~ 300 -700 km in horizontal dimension). They occurred more frequently over the two oceanic regions than over the maritime continent region for all three years. Furthermore, the largest clusters have the most pronounced interannual variation. They overwhelmingly preferred the WP region during the 1986-1987 warm ENSO event and switched to the IO region during the 1988-1989 cold ENSO event (Figures 8a and 8c).

The largest group of cloud clusters (> 300 km in horizontal dimension) are usually long lasting. *Chen et al.* [1996] and *Chen and Houze* [1997] showed that the lifetime of tropical cloud systems are generally proportional to their size, although there is a wide spread in the lifetime and size distribution. Most of the spatially large cloud clusters last from more than 10 hours up to several days. These large cloud clusters are also the main contributors to the diurnal cycle of total cold cloudiness over the ocean [*Chen and Houze*, 1997]. They occurred almost exclusively in the convectively active phases of the ISO [e.g., *Mapes and Houze*, 1993; *Chen et al.*, 1996]. The eastward-propagating feature in deep convection associated with the ISO disappeared when the large clusters were excluded in a time-longitude plot of cloud clusters in the work of *Mapes and Houze* [1993]. The large-scale environment conditions that give rise to these large, long-lasting cloud systems during the active phases of the ISO may be similar to that supporting anomalous convective activity during the warm ENSO event over the western Pacific in 1986-1987 and the cold event over the eastern Indian Ocean in 1988-1989.

6. Conclusions

The tropical equatorial deep convection exhibited significant interannual variability in the 4-month mean spatial patterns of percent high cloudiness (PHC) and rainfall.

The maximum convection was centered over the western central Pacific during the 1986-1987 warm ENSO event and switched to the Indian Ocean during the 1988-1989 cold ENSO event (Plates 1 and 2). The total domain-averaged PHC and the MSU-estimated precipitation as well as the fractional coverage of the PHC and precipitation, however, remained nearly constant for all three years over the Indo-Pacific warm-pool region (Figures 1 and 2). It suggests a near conservation of total amount of cold cloudiness and precipitation over the warm-pool region under the extreme conditions of the ENSO cycle of 1986-1989. This result indicates that the mechanism(s) controlling the total amount of deep convection over the warm pool may be independent of the ENSO cycle. However, the spatial shifting of location of convective activity center within the region, between the western central Pacific and the eastern Indian Ocean, and between the equatorial region and the SPCZ, is still the main reason for the global response to the convective variability related to the ENSO cycle.

Although deep convection prefers open, warm oceans, the large-scale distribution of deep convection does not always follow the SST distribution in the equatorial Indo-Pacific warm-pool region. Deep convection in the eastern Indian Ocean was much more frequent in 1988-1989 than the other two years, even though the SST did not change much. In fact, the warmest SST in the equatorial region was found over the western Pacific (145°-155°E) where convection was much less frequent than over the Indian Ocean in 1988-1989. In the western Pacific, on the other hand, the collocation of most frequent deep convection and the warmest SST is evident in 1986-1987 and 1987-1988. Deep convection in the region surrounding the maritime continent was less frequent than over the western Pacific or over the eastern Indian Ocean regardless of the SST distributions.

Each year, the intraseasonal oscillation (ISO) has a similar eastward zonal propagation, from the eastern Indian Ocean to the western Pacific, but with a large meridional variation from year to year. A Kelvin wave pattern was clearly evident when the deep convection was centered near the equator. However, the southward shift of the ISO during the cold ENSO event in 1988-1989 raises a question of whether the Kelvin-wave dynamics alone can explain the eastward propagation of the ISO since there is little Kelvin-wave-like disturbance in the equatorial region when the center of convective activity associated with the ISO is south of the equator.

The characteristics of the cloud clusters (defined by 208 K contour) showed an interesting interannual variation. While the spatially small cloud clusters have had similar size distributions for all three years, the largest cloud clusters occurred more frequently over the western central Pacific Ocean (Indian Ocean) during the warm (cold) ENSO event (Figure 8). This may explain the interannual seesaw pattern shown in both the 4-month mean PHC (Plate 1) and the MSU-estimated precipitation (Plate 2) and the unbalanced intraseasonal seesaw patterns in Figures 5-7. To explain this dramatic behavior of the convective anomaly, one should focus on the factors accounting for the horizontally extensive, long-lasting convective systems. Future modeling studies directed toward understanding the sustainability of convection and corresponding large-scale flow conditions will be important for the problem of interannual variability of deep convection over the warm pool.

Acknowledgments. We thank Chidong Zhang for his comments and suggestions during the course of this study, Gary Huitsing for processing part of the GMS IR data, Candace Gudmundson for editing the manuscript, and Kay Dewar for drafting assistance. Comments from two anonymous reviewers are also appreciated. This research was supported by a TOGA COARE grant from NOAA under Cooperative Agreement NA37RJ0198 (Joint Institute for the Study of the Atmosphere and Ocean contribution 433) and the NASA EOS grant NAGW-2633.

References

- Arkin, P. A., and B. N. Meisner, The relationship between large-scale convective rainfall and cold cloud over the western hemisphere during 1982-1984, *Mon. Weather Rev.*, **115**, 51-74, 1987.
- Charney, J. G., and A. Eliassen, On the growth of the hurricane depression, *J. Atmos. Sci.*, **21**, 68-75, 1964.
- Chen, S. S., and R. A. Houze, Jr., Diurnal variations and life-cycle of deep convective systems over the tropical Pacific warm pool, *J. R. Meteorol. Soc.*, **123**(B), 357-388, 1997.
- Chen, S. S., R. A. Houze, Jr., and B. E. Mapes, Multiscale variability of deep convection in relation to large-scale circulation in TOGA COARE, *J. Atmos. Sci.*, **53**, 1380-1409, 1996.
- Climate Analysis Center, *Climate Diagnostics Bulletin*, edited by V. E. Kousky, 50 pp., Nat'l. Oceanic and Atmos. Admin./NWS/NMC, Washington D.C., 1989.
- Emanuel, K. A., An air-sea interaction model of intraseasonal oscillations in the tropics, *J. Atmos. Sci.*, **44**, 2324-2340, 1987.
- Fu, R., A. D. Del Genio, and W. B. Rossow, Behavior of deep convective clouds in the tropical Pacific deduced from ISCCP radiances, *J. Clim.*, **3**, 1129-1152, 1990.
- Gill, A. E., Some simple solutions for heat-induced tropical circulations, *J. R. Meteorol. Soc.*, **106**, 447-462, 1980.
- Graham, N. E., and T. P. Barnett, Sea surface temperature, surface wind divergence, and convection over tropical oceans, *Science*, **238**, 657-659, 1987.
- Gutzler, D. S., Interannual fluctuations of intraseasonal variance of near-equatorial zonal winds, *J. Geophys. Res.*, **96**, 3173-3185, 1991.
- Hartmann, D. L., and J. R. Gross, Seasonal variability of the 40-50 day oscillation in wind and rainfall in the tropics, *J. Atmos. Sci.*, **45**, 2680-2702, 1988.
- Hartmann, D. L., H. H. Hendon, and R. A. Houze, Jr., Some implications of the mesoscale circulations in tropical cloud clusters for large-scale dynamics and climate, *J. Atmos. Sci.*, **41**, 113-121, 1984.
- Hayes, S. P., P. Chang, and M. J. McPhaden, Variability of the sea surface temperature in the eastern equatorial Pacific Ocean during 1986-1988, *J. Geophys. Res.*, **96**, 10553-10566, 1991.
- Hendon, H. H., A simple model of the 40-50 day oscillation, *J. Atmos. Sci.*, **45**, 569-584, 1988.
- Hendon, H. H., and B. Liebmann, Organization of convection within the Madden-Julian oscillation, *J. Geophys. Res.*, **99**, 8073-8083, 1994.
- Hendon, H. H., and M. L. Salby, The life cycle of the Madden-Julian Oscillation, *J. Atmos. Sci.*, **51**, 2225-2237, 1994.
- Hsu, H.-H., B. J. Hoskins, and F.-F. Jin, The 1985/86 intraseasonal oscillation and the role of the extratropics, *J. Atmos. Sci.*, **47**, 823-839, 1990.
- Hu, Q., and D. A. Randall, Low-frequency oscillations in radiative-convective systems, *J. Atmos. Sci.*, **51**, 1089-1099, 1994.
- Janowiak, J. E., and P. A. Arkin, Rainfall variations in the tropics during 1986-1989, as estimated from observations of cloud-top temperature, *J. Geophys. Res.*, **96**, 3359-3373, 1991.
- Kessler, W. S., M. C. Spillane, M. J. McPhaden, and D. E. Harrison, Scales of the variability in the equatorial Pacific inferred from the tropical atmosphere-ocean buoy array, *J. Clim.*, **9**, 2999-3024, 1996.
- Kiladis, G. N., and K. M. Weickmann, Extratropical forcing of tropical Pacific convection during northern winter, *Mon. Weather Rev.*, **120**, 1924-1938, 1992.
- Knutson, T. R., and K. M. Weickmann, 30-60 day atmospheric oscillations: Composite life cycles of convection and circulation anomalies, *Mon. Weather Rev.*, **115**, 1407-1436, 1987.
- Lau, K.-M., and P. H. Chan, Aspects of 40-50 day oscillation during the northern winter as inferred from outgoing longwave radiation, *Mon. Weather Rev.*, **113**, 1889-1909, 1985.
- Lau, K.-M., L. Peng, C.-H. Sui, and T. Nakazawa, Dynamics of super cloud clusters, westerly wind burst, 30-60 day oscillation, and ENSO: A unified view, *J. Meteorol. Soc. Jpn.*, **67**, 205-219, 1989.
- Lau, K.-M., T. Nakazawa, and C.-H. Sui, Observations of cloud cluster hierarchies over the tropical western Pacific, *J. Geophys. Res.*, **96**, 3197-3208, 1991.
- Madden, R., and P. Julian, Detection of a 40-50 day oscillation in the zonal wind in the tropical Pacific, *J. Atmos. Sci.*, **28**, 702-708, 1971.
- Madden, R., and P. Julian, Description of global scale circulation cells in the tropics with a 40-50 day period, *J. Atmos. Sci.*, **29**, 1109-1123, 1972.
- Mapes, B. E., and R. A. Houze, Jr., Cloud clusters and superclusters over the oceanic warm pool, *Mon. Weather Rev.*, **121**, 1398-1415, 1993.
- Matsumo, T., Quasi-geostrophic motions in the equatorial area, *J. Meteorol. Soc. Jpn.*, **44**, 25-43, 1966.
- Nakazawa, T., Tropical super clusters within intraseasonal variations over the western Pacific, *J. Meteorol. Soc. Jpn.*, **66**, 823-839, 1988.
- Neelin, J. D., I. M. Held, and K. H. Cook, Evaporation-wind feedback and low-frequency variability in the tropical atmosphere, *J. Atmos. Sci.*, **44**, 2341-2348, 1987.
- Newell, R. E., J. W. Kidson, D. G. Vincent, and G. J. Boer, *The General Circulation of the Tropical Atmosphere*, MIT Press, Cambridge, MA, vol. 2, 371 pp., 1974.
- Nogués-Paegle, J., B.-C. Lee, and V. E. Kousky, Observed modal characteristics of the intraseasonal oscillation, *J. Clim.*, **2**, 496-507, 1989.
- Ramage, C. S., *Monsoon Meteorology*, Academic Press, San Diego, CA, 296 pp., 1971.
- Ropelewski, C. F., and M. S. Halpert, Global- and regional-scale precipitation patterns associated with the high index phase of the Southern Oscillation, *Mon. Weather Rev.*, **115**, 1606-1626, 1987.
- Ropelewski, C. F., and M. S. Halpert, Precipitation patterns associated with the high index phase of the Southern Oscillation, *J. Clim.*, **2**, 268-284, 1989.
- Ropelewski, C. F., and P. D. Jones, An extension of the Tahiti-Darwin Southern Oscillation Index, *Mon. Weather Rev.*, **115**, 2161-2165, 1987.
- Rui, H., and B. Wang, Development characteristics and dynamic structure of tropical intraseasonal convection anomalies, *J. Atmos. Sci.*, **47**, 357-379, 1990.
- Salby, M. L., R. R. Garcia, and H. H. Hendon, Intraseasonal behavior of clouds, temperature, and motion in the tropics, *J. Atmos. Sci.*, **51**, 2344-2367, 1994.
- Spencer, R. W., Global oceanic precipitation from the MSU during 1979-1991 and comparisons to other climatologies, *J. Clim.*, **6**, 1301-1326, 1993.
- Sui, C.-H., and K.-M. Lau, Multiscale phenomena in the tropical atmosphere over the western Pacific, *Mon. Weather Rev.*, **120**, 407-430, 1992.
- Wang, B., Dynamics of tropical low-frequency waves: An analysis of the moist Kelvin wave, *J. Atmos. Sci.*, **45**, 2051-2065, 1988.
- Wang, B., and H. Rui, Synoptic climatology of transient tropical intraseasonal convection anomalies, *Meteorol. Atmos. Phys.*, **44**, 43-62, 1990.
- Weickmann, K. M., and S. J. S. Khalsa, The shift of convection from the Indian Ocean to the western Pacific Ocean during a 30-60 day oscillation, *Mon. Weather Rev.*, **118**, 964-978, 1990.
- Williams, M., and R. A. Houze, Jr., Satellite-observed characteristics of winter monsoon cloud clusters, *Mon. Weather Rev.*, **115**, 505-519, 1987.
- Zhang, C., Large-scale variability of atmospheric deep convection in relation to sea surface temperature, *J. Clim.*, **6**, 1898-1913, 1993.
- Zhang, C., Atmospheric intraseasonal variability at the surface in the western Pacific Ocean, *J. Atmos. Sci.*, **53**, 739-758, 1996.
- Zhu, B., and B. Wang, The 30-60-day convection seesaw between the tropical Indian and western Pacific oceans, *J. Atmos. Sci.*, **50**, 184-199, 1993.

Shuyi S. Chen, Department of Atmospheric Sciences, University of Washington, Box 351640, Seattle, WA 98195-1640. (e-mail: chen@atmos.washington.edu)

R. A. Houze, Jr. Department of Atmospheric Sciences, University of Washington, Box 351640, Seattle, WA 98195-1640. (e-mail: houze@atmos.washington.edu)

(Received February 28, 1997; revised August 1, 1997; accepted August 4, 1997.)